Geometrical-based Simulation of Drop-on-Demand 3D Inkjet Printing

WCMNM 2021

Ahmed Elkaseer[1*], Stella Schneider[1], Steffen Scholz[1,2,3]

[1]*Institute for Automation and Applied Informatics, Karlsruhe Institute of Technology, 76344 Karlsruhe, Germany*
[2]*Future Manufacturing Research Institute, College of Engineering, Swansea University, Swansea SA1 8EN, UK*
[3]*Karlsruhe Nano Micro Facility, Hermann-von-Helmholtz-Platz 1, 76344 Eggenstein-Leopoldshafen, Germany*
**ahmed.elkaseer@kit.edu*

Abstract

As additive manufacturing has evolved, 3D inkjet printing (IJP) has become a promising alternative manufacturing method able to manufacture functional multi-material parts in a single process. However, issues with part quality in terms of dimensional errors and lack of precision still restrict its industrial and commercial applications. This study aims at improving the dimensional accuracy of 3D IJP parts by developing an optimization-oriented simulation tool of droplet behaviour during the drop-on-demand 3D IJP process. The simulation approach takes into consideration the effect of droplet volume, resolution of processed TIFF image, contact angle of the ink on the solid substrate and coalescence performance of overlapping droplets, in addition to the number of printed layers. Following the development of the simulation tool using MATLAB, its feasibility was validated using already printed parts. The simulation results are found to be in a good agreement with the dimensions of the printed parts. The developed tool was then used to elucidate the effect of resolution of processed TIFF image and droplet diameter on the dimensional accuracy of 3D IJP parts.

Keywords: 3D Inkjet, Geometrical Simulation, Drop-on-demand, Dimensional accuracy, TIFF image resolution.

1. Introduction

Additive manufacturing (AM), which in contrast to conventional manufacturing techniques, constructs a part layer-by-layer, has undergone extensive development since its emergence. Different AM techniques have been developed and improved by individual researchers, and industrial laboratories, each focused on different materials or applications [1].

The key advantages of AM/3D printing are its limitless design freedom with regards to shape and materials, short lead times, the possibility of small batch sizes (even batches of just one) and customised parts. At first 3D printing was used mainly to produce prototypes during the development of new products. However, with improvements in the process and part quality, the potential to use it as part of a manufacturing process grew, especially in the automotive, aerospace, medical and electrical sectors. The possibility of including several materials in a single component, such as conductive, flexible, metal or ceramic materials or fibres, during a single production process was found to be relatively easily achieved with 3D printing, because no retooling is necessary which means parts can be optimised regarding their function instead of having to fit the manufacturing process [2].

As of today, AM comprises seven main technologies including, material extrusion, powder bed fusion and material jetting. One of the latter categories is 3D inkjet printing (IJP), a technology based on conventional inkjet printing which is found in many households and offices. 3D IJP is also called material jetting or polymer jetting. In the electrical sector 2D/3D IJP is widely applied to manufacture sensors and circuit boards, however it is also a promising technology for other sectors, such as the health or energy sectors due to its high resolution and resulting high scalability. Furthermore, in contrast to the commonly found powder-bed 3D printing technologies, the handling of multiple different materials is much more convenient and hence the creation of full-functional 2D and 3D parts with intricate features and geometries is relatively achievable [3].

To be able to use 3D IJP for industrial applications, it is crucial for the printed parts to be accurate and within agreed production tolerances. However, dimensional accuracy as well as other quality characteristics, such as surface roughness, are still an issue when it comes to 3D printing.

Unlike extrusion-based processes, such as in Fused Filament Fabrication (FFF), where the quality mostly depends on the material and the input parameters of the printer, in 3D IJP, also the CAD sliced part design in the form of TIFF files has a significant effect on the outcome. An important characteristic of these TIFF files is their resolution, which also helps to modify and optimise the process outcome.

In particular, a TIFF file with a higher resolution leads to less variation between segments printed by different nozzles of the printhead as well as smoother and clearer outlines of the part. However, this is a time-consuming printing process and increases the amount of material dispensed, thereby to some extent increasing the final dimensional error of the printed features when compared with the required CAD design.

The overall goal of this project is to develop an optimisation-oriented simulation tool using MATLAB to study the effect of the combination of resolution of the TIFF files and the drop diameter on the inkjet printing performance and hence to enable identifying optimal processing parameters, for high dimensional accuracy of inkjet-printed parts.

The paper is organised as follows. First, the theoretical background of the IJP and droplets is explained. Next, the development of the simulation tool, the validation of its feasibility and the results are presented and discussed. Finally, conclusions are drawn, and possible future work is proposed.

2. Theoretical Background

2.1. The 3D Inkjet Printing Process

In the 3D IJP process (see Fig. 1) a liquid photopolymer is jetted onto a substrate and immediately cured by an ultraviolet (UV) light source. Then the platform with the substrate moves down and a new layer of drops is applied, cured, and connected to the already built part.

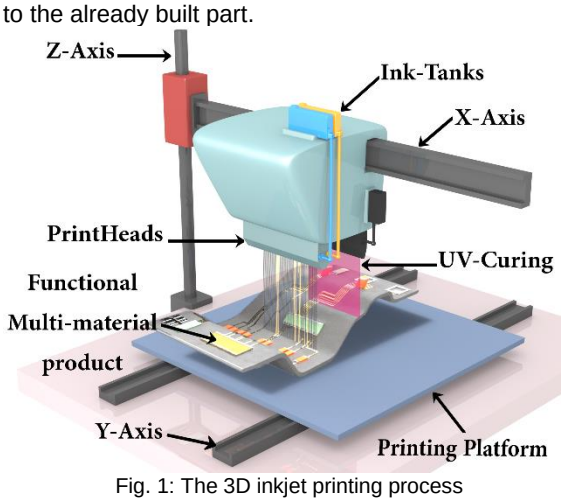

Fig. 1: The 3D inkjet printing process

The IJP process can be divided into two working principles regarding the ejection of the droplets. First, the continuous IJP mode where a continuous stream is ejected through the nozzle and due to Rayleigh instability separates into droplets. In contrast, using the second mode, drop-on-demand (DOD), it is possible to eject the droplets when needed, controlled by digital signals and hence to place them at an exact spot on the substrate by moving either the substrate or the inkjet printing head [4]. To eject the droplets on demand from the nozzle a thermal or piezoelectric actuator controlled by an actuation pulse voltage can be used. In the case of the latter the voltage causes a deformation of the piezoelectric actuator. Hence in both methods a reduction of chamber volume occurs, so that the ink is compressed and forced to eject a drop [3].

2.2. Physics of Droplets in Inkjet Printing

Two crucial properties of fluids, i.e., inks, for the IJP are their surface tension γ and viscosity η. The surface tension is the dominant force responsible for the drop adopting a spherical shape if it is in contact with only the ambient air and is not significantly influenced by other forces such as gravitational or aerodynamic. The viscosity can be described as the resistance of a liquid to shear deformation or flow. Due to a cohesive intermolecular force, friction can be said to occur between layers of the fluid moving relative to each other [5].

When a droplet impacts onto a substrate it will oscillate before it forms its capillary-driven equilibrium shape, which is a spherical cap. The diameter of this spherical cap can be determined from the initial droplet diameter d_0 and the equilibrium contact angle θ_{eqm} by Eq. 1 [6, 7].

$$d_{eqm} = d_0 * \sqrt[3]{\frac{8}{\tan\frac{\theta_{eqm}}{2} * \left(3 + \tan^2\frac{\theta_{eqm}}{2}\right)}} \qquad (1)$$

A major factor in the equations representing a fluid on a solid substrate is the contact angle, which depends on the surface tension between the liquid and the solid, as found from the Young equation [8].

When two drops coalesce, they first connect over a meniscus bridge which then expands until the drops fully merge into one hemispherical spherical cap provided that the drop spacing, i.e. the centre-to-centre distance is smaller than the drop diameter [9]. This process is also applicable to the formation of a line of drops. If several drops are deposited onto the substrate linearly, they will form a liquid line which has a hemispherical cross-section. The width w of this line will depend on the initial droplet diameter d_0, the droplet spacing p and the contact angle θ_{eqm} (see Eq. 2) [7].

$$w = \sqrt{\frac{2\pi {d_0}^3}{3p\left(\frac{\theta_{eqm}}{\sin^2\theta_{eqm}} - \frac{\cos\theta_{eqm}}{\sin\theta_{eqm}}\right)}} \qquad (2)$$

The stability of the line depends in part on the droplet spacing. If the droplets are deposited too far apart or too close to each other the line becomes discontinuous or bulges occur. This bulging of the line and the following instability was examined by Duineveld [10] who investigated conditions for unstable lines and how to describe their shape and geometry in terms of mathematical models.

In order to describe the geometry of a bulge, first its shape regarding the curvature in line with the ridge is shown, for a top view of the line, see Figure 2a. The bulge can be seen as a trimmed circle with radius R which intersects the ridge of the line at an angle α. The outline of the circle is defined by Equations 3 and 4.

$$b(x) = b_0 + 2\left(\sqrt{R^2 - x^2} - R\cos\alpha\right), \qquad (3)$$

$$x_0 = R\sin\alpha \qquad (4)$$

To describe the surface of the bulge, as well as any surface of an ideal bead, Equation 5 can be used. For the bulge, $r(x)$ is defined by equation 6 and hence for an ideal bead $b(x) = w$ (see Figure 2b).

$$z(x,y) = \sqrt{r^2(x) - y^2} - r(x)\cos\theta_a \qquad (5)$$

$$r(x) = \frac{b(x)}{2\sin\theta_a} \qquad (6)$$

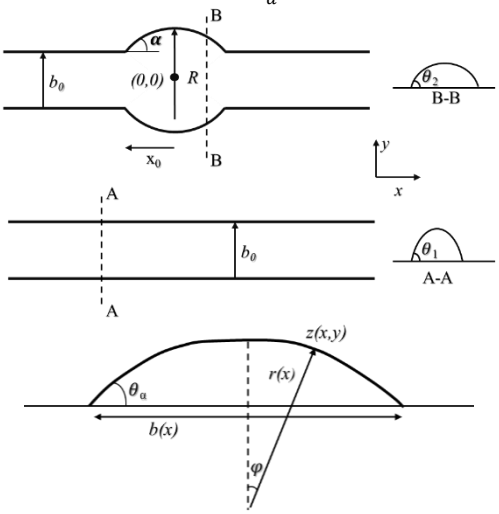

Fig. 2: a) Top view of a line with a bulge and a stable line with constant width b0, b) Cross-section of a bulge [10]

2.3. Tagged Image File Format

Since in this work only bi-level TIFFs are of relevance, these file formats are described in detail below. Bi-level images contain only two colours, in this

case black and white, which are identified by the numbers zero and one. Depending on the photometric interpretation either white or black is displayed as zero. One of the most crucial properties of a TIFF is the length and width of its array of pixels, i.e., the number of rows and columns. When this property is combined with the next important characteristic, namely the resolution, the size of the picture can be calculated. The resolution states the number of pixels, also called dots per unit length, most commonly referred to as dots per inch (dpi). It should be noted that different resolutions for the width and length are possible, referred to as X-Resolution and Y-Resolution [11].

3. Simulation Tool and Validation

3.1. Simulation Tool

To get a general understanding of how the tool works and the necessary steps, the structure and work flow of the simulation tool is displayed in Figure 3 by a flowchart.

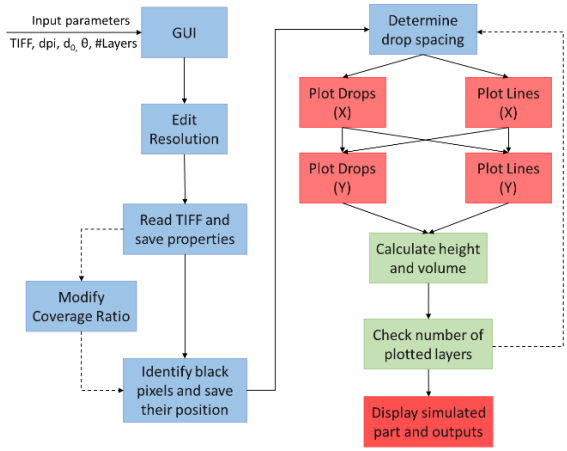

Fig. 3. Flowchart of the developed simulation tool

The workflow of the tool can generally be divided into three main groups: Data preparation (blue), plotting and displaying (red) and processing of the generated data (green).

After the necessary input parameters are inserted through the GUI, in a first step the resolution of the TIFF is modified to that desired. Next, the TIFF data is read into the program and properties such as the new resolution and the pixel matrix are saved. Then all the black pixels, which will later be covered with a drop are identified and their positions saved.

Using these positions, the distance between neighbouring black pixels and hence the droplet spacing is determined and also saved. Depending on the droplet spacing, first all single drops or drop lines in the X-direction are plotted, followed by those in the Y-direction. To be able to add further layers, the layer height needs to be calculated and the overall drop volume ascertained. If the required number of layers is not reached, the tool goes back to plotting the drops based on their drop spacing for the next layer. When all layers have been plotted, the final result is displayed and relevant output variables are given, such as the height of a single layer.

In Figure 4, an example of a simulated dogbone layer is shown. On the left-hand side (a) the overall result can be seen, when zooming in closer, the surface and shape of the edges is seen (b). In picture (c) a cross section through the xy-plane near the bottom is shown, showing how the lines are plotted and that the x- and y-lines overlap each other to approximate the planar surface of a drop array. By implementing a radius at the end of each line, corners and edges are more detailed and closer to reality, in contrast to rectangular line base shapes.

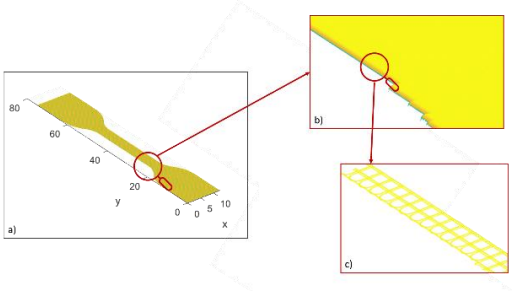

Fig. 4. Example of a simulated dogbone structure

In Figure 5, simulations of different shapes and parts are illustrated. Pictures a) and b) visualise a single simulated layer. In picture b) the effect of the pixels is clearly detectable at the edges of the triangle and also in the shape of the circle in the middle. Pictures c) and d) show a more practical usage, with picture c) displaying the etching of a circuit board and picture d) a basic 3D part. In the latter the layer structure and their stacking is visible.

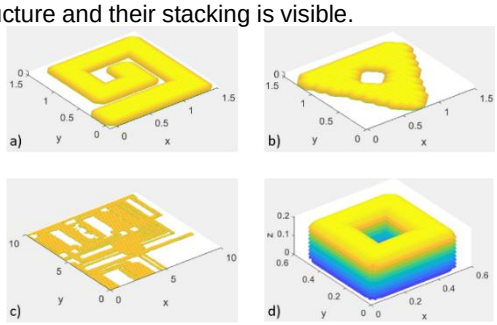

Fig. 5. Simulation of different shapes with the developed simulation tool

3.2. Validation of Results

To validate the results produced by the simulation tool, they were compared with printed parts by inserting the same parameters which were applied to the parts into the simulation tool. Some of those input parameters were for the printing of the “dogbone” and could be obtained from an xml-file, which contains the values and instructions for the 3D IJP machine. Others needed to be calculated.

- X-resolution dpi_x: 360 dpi
- Y-resolution dpi_y: 360.2837 dpi
- Number of layers: 100
- Layer Height: 17.2 µm
- Drop Diameter d_0: 54.6701 µm
- Contact Angle θ_{eqm}: 34.5019°

The dimensions of the printed dogbone were ascertained as shown in Figure 6 using a digital calliper at three printed parts.

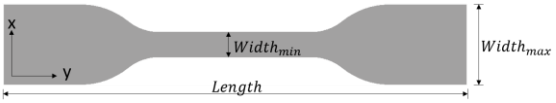

Fig. 6. Dimensions of the dogbone part to be used for the experimental validation.

In Figure 7 the metrics ascertained from the printed parts and the simulation tool are shown, as well as the ideal metric values according to the TIFF.

It can be seen that the values are quite close to each other and differ only by several microns. Moreover, the values simulated by the developed tool are consistently higher than those measured on the printed parts, whereas the original value from the TIFF mostly lie below or equal those on the printed dogbones. From the “dogbone” and the respective xml-file a layer height of 17.2 µm was extracted. The simulation tool produced a layer height of 16.7 µm, which is 0.5 µm lower than the desired height.

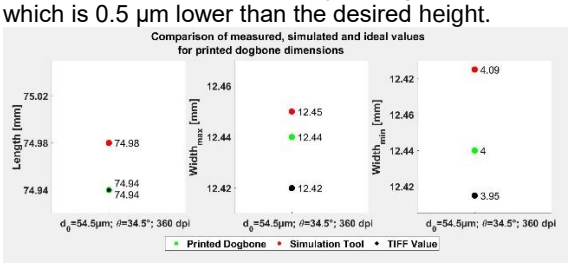

Fig. 7. Results of the validation using already printed dogbone part

It is found that the simulated dimensions (length and width) were larger than the ones of the printed dogbone structures. The reason for these higher values could be that the time until the material is cured was not considered when implementing the simulation. Hence, it could be that the material is cured with the UV-lamp before the droplets reach their equilibrium shape. This means that the contact angle would be higher, also the drop height, and the droplets would spread less. How fast the droplets spread depends among other factors on the viscosity of the ink used. These factors should be optimized to obtain highly accurate printed parts.

Moreover, in the simulation tool only drop lines are created and not drop arrays. But it could be assumed that when placing several drop lines next to each other that those would coalesce and tighten up in order to form a planar surface [12] (see Figure 8).

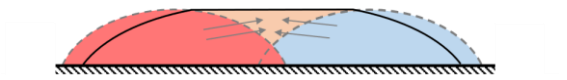

Fig. 8. Cross section of two coalescing drop lines and the resulting surface

Looking at the validation results it can be said that the developed simulation tool produces values which are close to the measured dimensions of printed parts and values produced by similar software programs. Nevertheless, there seem to be deviations, which might be reduced by including the curing time and a more precise simulation of the drop arrays. However, some differences between the values will always be found due to printer inaccuracies and tolerances, as well as different software packages and application principles. Thus, one can say that the simulation tool is close to the dimensions encountered in reality and applicable to the 3D IJP process, and could be applied to the printing process, especially to get a first impression about the effects of the parameter settings.

4. Conclusions

In this paper the development of a simulation tool and its validation for 3D IJP was presented. An insight into 3D IJP and the physics of droplets were given. The main characteristics of a TIFF images were explained. The working principle of the simulation tool were introduced, and the results of the validation discussed. The main results of this work are:

- A simulation tool has been presented which models the behaviour of ink droplets in the 3D inkjet printing process on a substrate before curing
- A validation and applicability evaluation of the simulation tool shows general agreement between simulations done with the tool and printed parts.

It can be concluded that the simulation tool aids the visualisation of the drop behaviour on the substrate as well as the effects of resolution and drop diameter. Through the use of the tool it came clear that the resolution of the input TIFF file plays a significant role in the outcome and quality of the printed part. By using the tool, possible errors and inaccuracies can be detected before the printing process is started and hence can be avoided.

Acknowledgements

This work was carried out with the support of the Karlsruhe Nano Micro Facility (KNMFi, www.knmf.kit.edu), a Helmholtz Research Infrastructure at Karlsruhe Institute of Technology (KIT, www.kit.edu) and under the Helmholtz Research Programme STN (Science and Technology of Nanosystems) at KIT.

References

[1] A. Charles, et al., "Effect of Process Parameters on the Generated Surface Roughness of Down-Facing Surfaces in Selective Laser Melting", Applied Sciences, 2019; 9: 1256.

[2] A. Elkaseer, et al., "Experiment-Based Process Modeling and Optimization for High-Quality and Resource-Efficient FFF 3D Printing", Applied Sciences, 2020; 10.

[3] J. Huang, et al., "Unsupervised learning for the droplet evolution prediction and process dynamics understanding in inkjet printing", Additive Manufacturing, 2020; 35.

[4] D.-W. Cho, et al., Inkjet-based 3D printing, in Organ Printing, Morgan & Claypool Publishers: 2015, 3.1-3.7.

[5] I.M. Hutchings, et al., Introductory Remarks, in Fundamentals of Inkjet Printing: The Science of Inkjet and Droplets, Wiley-VCH Verlag GmbH & Co. KGaA.: 2015, 1-12.

[6] J. Stringer, et al., "Formation and Stability of Lines Produced by Inkjet Printing", Langmuir, 2010; 26: 10365-10372.

[7] B. Derby, "Inkjet Printing of Functional and Structural Materials: Fluid Property Requirements, Feature Stability, and Resolution", Annual Review of Materials Research, 2010; 40: 395-414.

[8] S. Jung, et al., Drops on Substrates, in Fundamentals of Inkjet Printing: The Science of Inkjet and Droplets, Wiley-VCH Verlag GmbH & Co. KGaA.: 2015, 199-218.

[9] R. Li, et al., "Coalescence of two droplets impacting a solid surface", Experiments in Fluids, 2010; 48: 1025-1035.

[10] P.C. Duineveld, "The stability of ink-jet printed lines of liquid with zero receding contact angle on a homogeneous substrate", Journal of Fluid Mechanics, 2003; 477: 175-200.

[11] Aldus Developers Desk, "TIFF - Revision 6.0", 1992.

[12] W. Zhou, et al., "Lattice Boltzmann simulations of multiple-droplet interaction dynamics", Physical review. E, 2014; 89.